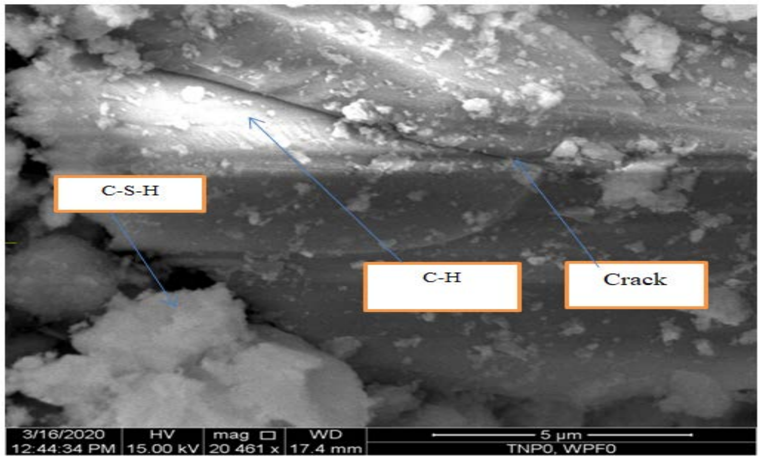

Figure 1 (a): SEM micrographs of unmodified (CCM) sample

Fig. 1 (b) shows FE-SEM image of (0.5% TNP + 0.4 % WPF). The image showed a large amount of gel like materials existence, which is C-S-H that is responsible to fill the pores in the concrete microstructures to enhance the concrete properties. Uniformly dispersed TiO_2 nanoparticles accelerated the formations of C-S-H components in the whole concrete structure by controlling the crystallization process and hence, restricted the growth of $Ca(OH)_2$. TiO_2 nanoparticle serves as the nuclei, which will change the hydration process, and thus, leading to the morphology change of the hydration products. Furthermore, it could be able to fill the nano-sized pores in the amorphous cementitious hydration products to reduce permeability of aggressive environmental conditions, and tend to increase density C-S-H phase.

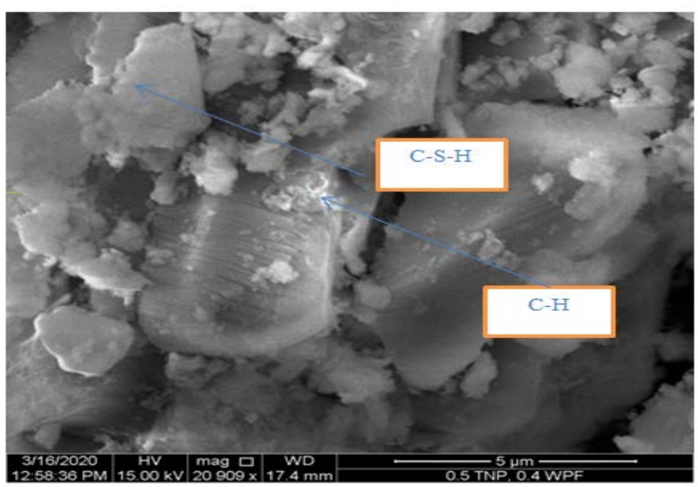

Figure 1 b: SEM micrograph of 0.5 % TNP + 0.4 % WPF modified sample

FE-SEM micrograph of 1 % TNP modified concrete shown in Figure 1 (c) indicated large amount of gel like material, which is C-S-H generated. At the same time, crystallization of concrete components is very limited. The partial replacement of cement with TNP accelerated the hydration process in concrete, and helped to generate more C-S-H gel like material, which is responsible for improving durability and mechanical properties.

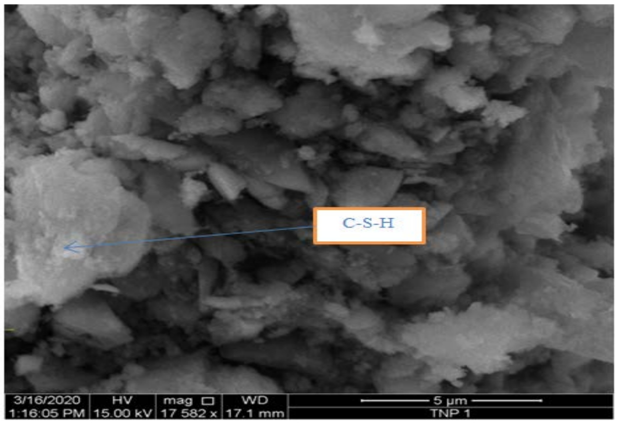

Figure 1 (c): SEM micrograph of 1% TNP modified concrete

Figure 2 shows the XRD results for the CCM and concrete modified with TiO_2 nanoparticles and waste plastic fiber. In case of CCM, the samples have shown unhydrated C-H phases at (2Θ = 10.90^o, 29.44^o, and 29.46^o). However, these phases were suppressed (absent) for the modified (1 % TNP and 0.5 % TNP and 0.4 % WPF) samples. Furthermore, the CCM samples have the unhydrated C_3S and C_2S phases at (2Θ = 26.72^o) and (2Θ = 28.76^o), respectively. In case of TiO_2 nanoparticles modified samples, the hydrated C-S-H phases appeared at (2Θ = 47.14^o and 50.26^o) and the C-H phases that appeared in CCM sample at (2Θ = 10.90^o) was possibly converted into C-S-H phase in both (0.5 % TNP & 0.4 % WPF) and (1% TNP) samples.

The SiO_2 (quartz) compositions peaks appeared for all the diffractograms at (2Θ = 18.17^o, 29.91^o, and 31.18^o). The modifications of concrete materials with the partial replacement of cement with TNP and sand with WPF, ensured with the increase in the peak corresponding to C-S-H phases, and simultaneously reduction in the C-H, C_3S and C_2S phases. This could be attributed due to the enabling of hydration reactions in the cement paste, and the consumption of $(CaOH)_2$, C_2S and C_3S to form an extra C-S-H gels like material.

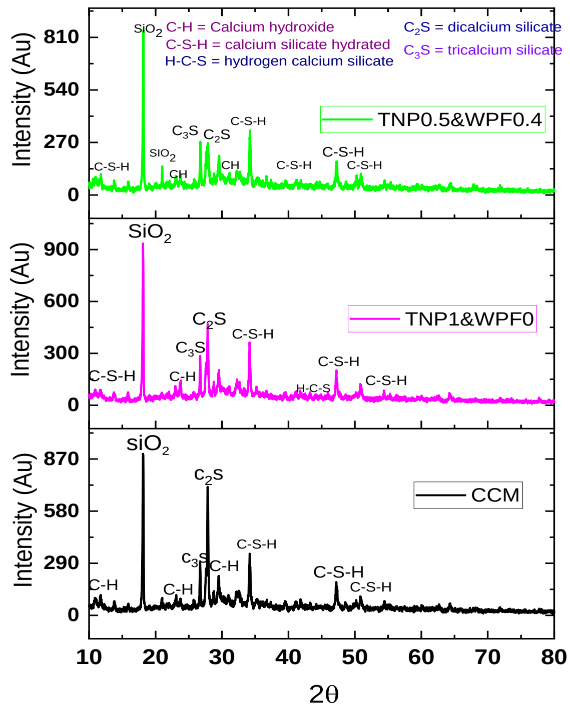

Figure 2: XRD spectra of unmodified (CCM), and modified with 1% TNP and (0.5% TNP & 0.4% WPF) modified samples

(Figure 3), the thermo-gravimetric tests were also done to find the thermal stability of concrete materials. The TGA-DSC tests were conducted starting from room temperature to 800°C temperature ranges with increasing heating rate of 10°C/minute. The weight loss has been appeared up to about 100 °C was due to dehydration and moisture removal from the sample. The maximum weight loss has recorded at the temperature of 426.43 °C and 433.85 °C for CCM; and TNP and WFP modified samples due to dehydroxylation and other hydration products, respectively. The mass loss occurred at about 668°C was attributed to the decarbonation of calcite ($CaCO_3$) in cement paste.

The DSC plot exhibited three main exothermic events during the entire heating process. The first occurs on the temperatures range from the onset to 77 °C for the unmodified sample, and at 82 °C for the modified samples. These weight losses were resulted from the dehydration and evaporation of moisture contents. Similarly, for modified concrete, (fig 3.6b), exhibits three main exothermic events. The first exothermic reaction occurred from onset temperature to 106 °C. At 106 °C, heat is absorbed - endothermic transition. From 106 °C to 380 °C, crystallization occurred - an exothermic event. Finally, bond formations occurred. At temperature of 380 °C again melting take place. Furthermore, from 380 °C to 600 °C crystallization undertakes.

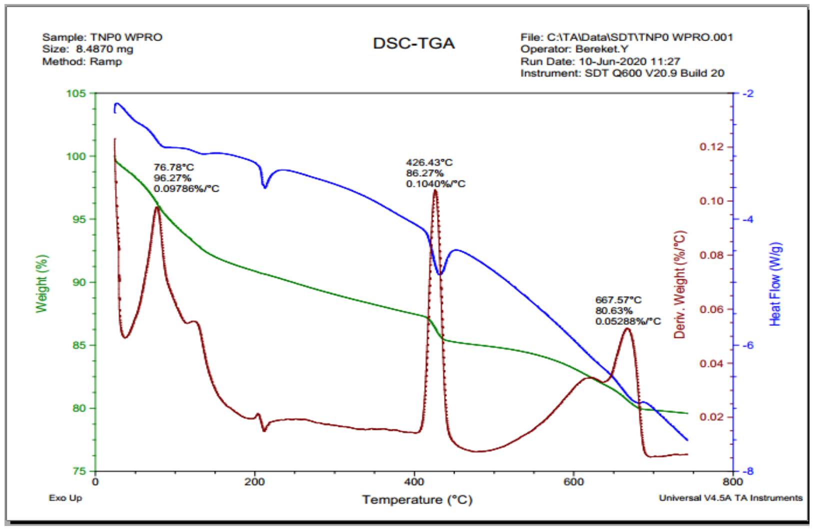

Figure 3a: DSC-TGA result of unmodified concrete materials

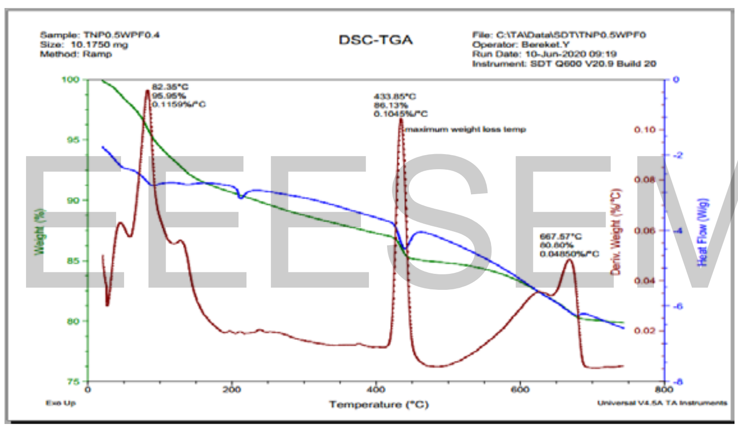

Figure 3 b: DSC-TGA results of 0.5 % TNP & 0.4 % WPF modified concrete

Conclusions

In this paper, the combined effects of TiO_2 nanoparticles and waste plastic fiber with various compositions were investigated. The results from mechanical tests indicated that both TiO_2 nanoparticles and waste plastics fibers have improved the mechanical properties like compressive strength, splitting tensile strength and maximum load resistance of the concrete materials. In addition, all of the modified concrete showed enhanced properties with respect to water permeability. In particular, 0.5 % TNP + 0.4 % WFP sample showed remarkable improvement in all aspects. For instance, the compressive strength of both TiO_2 nanoparticles and waste plastic fibers modified concrete after 28 days of curing time showed 29.01 to 39.05 MPa. Similarly, the split tensile strength showed increment from 5.14 to 9.52 MPa.

From the morphological study; the microstructure of modified concrete showed well-formed gels like materials, this is the indication of the existence of C-S-H. The thermal analysis of modified concrete indicated weight loss appeared at relatively higher temperatures than unmodified concrete sample. Furthermore, the XRD test result of unmodified concrete has shown the existence of various unhydrated phases like C-H, C_2S, C_3S and other unhydrated phases. Contrarily, the presence of hydrated phases, such as C-S-H gel like phases have confirmed modification in concrete materials. In general, the concrete materials modified with TiO_2 nanoparticles and waste plastics fiber has clearly shown developed cracks-resistance behavior in concrete structure.

Acknowledgement

The authors greatly acknowledged "Africa Center of Excellence in Materials, Product Development and Nanotechnology (MAPRONANO ACE) supported by the World Bank and hosted by the College of Engineering, Design, Art and Technology (CEDAT) at Makerere University, Kampala Uganda for provision of fund to accomplish this paper. The authors interested to acknowledge "Chemical and Construction Inputs Industry. Development Institute, for provision of M.Sc. scholarship and financial support. We acknowledge Addis Ababa Institute of Technology, Civil Engineering department materials testing laboratory for creating of an opportunity to conduct laboratory work successfully and testing of mechanical properties and durability. Also, we thank Mr. Demeke Tesfaye (Lab Assistance, Adama Science and Technology University) in supporting the acquisition of X-ray Diffraction. Furthermore, also we thank Mr. Habitamu Zewud (Lab Assistance, Addis Ababa Science and Technology University) for the acquisition of FE-SEM images.

Finally, we acknowledge Mr. Bereket Yihes (Lab Assistance, Ethiopia Leather Institute) for the acquisition of DSC/TGA analysis.

References

1. A, V. and S. M (2017). "Usage of Carbon nanotubes and nano fibers in cement and concrete: A review." International Journal of Engineering and Technology 9(2): 564-569
2. Alani, A. H., et al. (2019). "Durability performance of a novel ultra-high-performance PET green concrete (UHPPGC)." Construction and Building Materials 209: 395-405.
3. Bhogayata, A. C. and N. K. Arora (2018). "Workability, strength, and durability of concrete containing recycled plastic fibers and styrene-butadiene rubber latex." Construction and Building Materials 180: 382-395.

4. Ceran, Ö. B., et al. (2019). "Effects of dispersed and powdered silver nanoparticles on the mechanical, thermal, electrical and durability properties of cementitious composites." Construction and Building Materials 222: 152-167.
5. Diab, A. M., et al. (2019). "Effect of nanomaterials additives on performance of concrete resistance against magnesium sulfate and acids." Construction and Building Materials 210: 210-231.
6. Foti, D. (2011). "Preliminary analysis of concrete reinforced with waste bottles PET fibers." Construction and Building Materials 25(4): 1906-1915.
7. Han, Wang et al. (2017). "Properties and modification mechansm of nano-zirconia filled reactive powder concrete" 426-434
8. Harilal, M., et al. (2019). "High performance green concrete (HPGC) with improved strength and chloride ion penetration resistance by synergistic action of fly ash, nanoparticles and corrosion inhibitor." Construction and Building Materials 198: 299-312.
9. Ma, Li et al. (2015). "Effects of Nano-TiO2on the Toughness and Durability of Cement-Based Material." Advances in Materials Science and Engineering 2015: 1-10.
10. Mustafa, M. A.-T., et al. (2019). "Effect of partial replacement of sand by plastic waste on impact resistance of concrete: experiment and simulation." Structures 20: 519-526.
11. Paul, S. C., et al. (2018). "Properties of cement-based composites using nanoparticles: A comprehensive review." Construction and Building Materials 189: 1019-1034.
12. Pereira, E. L., et al. (2017). "Optimization of mechanical properties in concrete reinforced with fibers from solid urban wastes (PET bottles) for the production of ecological concrete." Construction and Building Materials 149: 837-848.
13. Pietrzak, A., et al. (2016). "Application of Titanium Dioxide in Cement and Concrete Technology." Key Engineering Materials 687: 243-249.
14. Vishwakarma, V. and D. Ramachandran (2018). "Green Concrete mix using solid waste and nanoparticles as alternatives – A review." Construction and Building Materials 162: 96-103.
15. Wu, Z., et al. (2016). "Effects of different nanomaterials on hardening and performance of ultra-high strength concrete (UHSC)." Cement and Concrete Composites 70: 24-34.
16. Xu, Xie., et al. (2018). "Environmental resistance of cement concrete modified with low dosage nano particles." Construction and Building Materials 164: 535-553.